

PARTICLE INTERFEROMETRY IN HEAVY-ION COLLISIONS

ULRICH HEINZ

*Institut für Theoretische Physik, Universität Regensburg,
D-93040 Regensburg, Germany*

Abstract

By measuring hadronic single-particle spectra and two-particle correlations in heavy-ion collisions, the size and dynamical state of the collision fireball at freeze-out can be reconstructed. I discuss the relevant theoretical methods and their limitations. By applying the formalism to recent pion correlation data from Pb+Pb collisions at CERN we demonstrate that the collision zone has undergone strong transverse growth before freeze-out (by a factor 2-3 in each direction), and that it expands both longitudinally and transversally. From the thermal and flow energy density at freeze-out the energy density at the onset of transverse expansion can be estimated from conservation laws. It comfortably exceeds the critical value for the transition to color deconfined matter.

1 Introduction

In the last few years a large body of evidence has been accumulated that the hot and dense collision region in ultrarelativistic heavy ion collisions thermalizes and shows collective dynamical behaviour. This evidence is based on a comprehensive analysis of the hadronic single particle spectra. It was shown that all available data on hadron production in heavy ion collisions at the AGS and the SPS can be understood within a simple model which assumes locally thermalized momentum distributions at freeze-out, superimposed by collective hydrodynamical expansion in both the longitudinal and transverse directions [1, 2]. The collective dynamical behaviour in the transverse direction is reflected by a characteristic dependence of the inverse slope parameters of the m_{\perp} -spectra (“effective temperatures”) at small m_{\perp} on the hadron masses [1]. New data from the Au+Au and Pb+Pb systems [3] support this picture and show that the transverse collective dynamics is much more strongly exhibited in larger collision systems than in the smaller ones from the first rounds of experiments. The amount of transverse flow also appears to increase monotonically with collision energy from GSI/SIS to AGS energies, but may show

signs of saturation at the even higher SPS energy [3].

The extraction of flow velocities and thermal freeze-out temperatures from the measured single particle spectra relies heavily on model assumptions [1]. There have been alternative suggestions to explain the observed features of the hadron spectra without invoking hydro-flow [4, 5]. The single-particle spectra are ambiguous because they contain no direct information on the space-time structure and the space-momentum correlations induced by collective flow. In terms of the phase-space density at freeze-out (“emission function”) $S(x, p)$ the single-particle spectrum is given by $E dN/d^3p = \int d^4x S(x, p)$; the space-time information in S is completely washed out by integration. Thus, on the single-particle level, comprehensive model studies are required to show that a simple hydrodynamical model with only a few thermodynamic and collective parameters can fit all the data, and additional consistency checks are needed to show that the extracted fit parameter values lead to an internally consistent theoretical picture. The published literature abounds with examples demonstrating that without such consistency checks the theoretical ambiguity of the single particle spectra is nearly infinite.

This is the point where Bose-Einstein correlations between the momenta of identical particle pairs provide crucial new input. They give direct access to the space-time structure of the source *and* its collective dynamics. In spite of some remaining model dependence the set of possible model sources can thus be reduced dramatically. The two-particle correlation function $C(q, K)$ is usually well approximated by a Gaussian in the relative momentum q whose width parameters are called “HBT (Hanbury Brown-Twiss) radii”. It was recently shown [6]-[8] that these radius parameters measure certain combinations of the second central space-time moments of the source. In general they mix the spatial and temporal structure of the source in a nontrivial way [7], and the remaining model dependence enters when trying to unfold these aspects.

Collective dynamics of the source leads to a dependence of the HBT radii on the pair momentum K ; this has been known for many years [10, 11], but was recently quantitatively reanalyzed, both analytically [7, 8, 9, 12] and numerically [13, 14]. The velocity gradients associated with collective expansion lead to a dynamical decoupling of different source regions in the correlation function, and the HBT radii measure the size of the resulting “space-time regions of homogeneity” of the source [11, 9] around the point of maximum emissivity for particles with the measured momentum K . The velocity gradients are smeared out by a thermal smearing factor arising from the random motion of the emitters around the fluid velocity [7]. Due to the exponential decrease of the Maxwell-Boltzmann distribution, this smearing factor shrinks

with increasing transverse momentum K_{\perp} of the pair, which is the basic reason for the K_{\perp} -dependence of the HBT radii.

Unfortunately, other gradients in the source (for example spatial and temporal temperature gradients) can also generate a K -dependence of the HBT radii [7, 12]. Furthermore, the pion spectra in particular are affected by resonance decay contributions, but only at small K_{\perp} . This may also affect the HBT radii in a K_{\perp} -dependent way [15, 16]. The isolation of collective flow, in particular transverse flow, from the K_{\perp} -dependence of the HBT radii thus requires a careful study of these different effects.

We studied this K -dependence of the HBT radii within a simple analytical model for a finite thermalized source which expands both longitudinally and transversally. For presentation I use the Yano-Koonin-Podgoretskii (YKP) parametrization of the correlator which, for sources with dominant longitudinal expansion, provides an optimal separation of the spatial and temporal aspects of the source [8, 14]. The YKP radius parameters are independent of the longitudinal velocity of the observer frame. Furthermore, in all thermal models without transverse collective flow, they show perfect M_{\perp} -scaling (in the absence of resonance decay contributions). Only the transverse gradients induced by a non-zero transverse flow can break this M_{\perp} -scaling, causing an explicit dependence on the particle rest mass. This allows for a rather model-independent identification of transverse flow from accurate measurements of the YKP correlation radii for pions and kaons. High-quality data should also allow to control the effects from resonance decays.

Due to space limitations, I will be extremely selective with equations, figures and references. A comprehensive and didactical discussion of the formalism and a more extensive selection of numerical examples can be found in Ref. [17] to which I refer the reader for more details.

2 The source model

For our study we use the model of Ref. [8] for an expanding thermalized source:

$$S(x, K) = \frac{M_{\perp} \cosh(\eta - Y)}{8\pi^4 \Delta\tau} \exp\left[-\frac{K \cdot u(x)}{T(x)} - \frac{(\tau - \tau_0)^2}{2(\Delta\tau)^2} - \frac{r^2}{2R^2} - \frac{(\eta - \eta_0)^2}{2(\Delta\eta)^2}\right] \quad (1)$$

Here $r^2 = x^2 + y^2$, the spacetime rapidity $\eta = \frac{1}{2} \ln[(t + z)/(t - z)]$, and the longitudinal proper time $\tau = \sqrt{t^2 - z^2}$ parametrize the spacetime coordinates x^{μ} , with measure $d^4x = \tau d\tau d\eta r dr d\phi$. $Y = \frac{1}{2} \ln[(E_K + K_L)/(E_K - K_L)]$ and $M_{\perp} = \sqrt{m^2 + K_{\perp}^2}$ parametrize the longitudinal and transverse components

of the pair momentum \vec{K} . $T(x)$ is the freeze-out temperature, $\sqrt{2}R$ is the transverse geometric (Gaussian) radius of the source, τ_0 its average freeze-out proper time, $\Delta\tau$ the mean proper time duration of particle emission, and $\Delta\eta$ parametrizes [7] the finite longitudinal extension of the source. The expansion flow velocity $u^\mu(x)$ is parametrized as

$$u^\mu(x) = (\cosh \eta \cosh \eta_t(r), \sinh \eta_t(r) \vec{e}_r, \sinh \eta \cosh \eta_t(r)), \quad (2)$$

with a boost-invariant longitudinal flow rapidity $\eta_l = \eta$ ($v_l = z/t$) and a linear transverse flow rapidity profile

$$\eta_t(r) = \eta_f \left(\frac{r}{R} \right). \quad (3)$$

η_f scales the strength of the transverse flow. The exponent of the Boltzmann factor in (1) can then be written as

$$K \cdot u(x) = M_\perp \cosh(Y - \eta) \cosh \eta_t(r) - \vec{K}_\perp \cdot \vec{e}_r \sinh \eta_t(r). \quad (4)$$

For vanishing transverse flow ($\eta_f = 0$) the source depends only on M_\perp , and remains azimuthally symmetric for all K_\perp .

3 HBT radius parameters

From the source function (1) the correlation function is calculated via the relation [18]

$$C(\vec{q}, \vec{K}) \approx 1 + \frac{|\int d^4x S(x, K) e^{iq \cdot x}|^2}{|\int d^4x S(x, K)|^2} = 1 + \frac{|\int d^4x S(x, K) e^{i\vec{q} \cdot (\vec{x} - \vec{\beta}t)}|^2}{|\int d^4x S(x, K)|^2}. \quad (5)$$

Here $q = p_1 - p_2$, $K = (p_1 + p_2)/2$ are the relative and average 4-momenta of the boson pair. The quality of the approximation in (5) is discussed in [7]. Since p_1, p_2 are on-shell and thus $K \cdot q = 0$, $q^0 = \vec{\beta} \cdot \vec{q}$ (with $\vec{\beta} = \vec{K}/K^0 \approx \vec{K}/E_K$) is not an independent variable and can be eliminated (second equality in (5)). Therefore the Fourier transform in (5) cannot be inverted without a model for $S(x, K)$. This is the reason for the model dependence of the interpretation of HBT correlation data mentioned in the Introduction.

We use a cartesian coordinate system with the z -axis along the beam direction and the x -axis along \vec{K}_\perp . Then $\vec{\beta} = (\beta_\perp, 0, \beta_l)$. We assume an azimuthally symmetric source (impact parameter ≈ 0) and write $C(\vec{q}, \vec{K})$ in the YKP parametrization [8, 14]:

$$C(\vec{q}, \vec{K}) = 1 + \exp \left[-R_\perp^2 q_\perp^2 - R_\parallel^2 (q_l^2 - (q^0)^2) - (R_0^2 + R_\parallel^2) (q \cdot U)^2 \right]. \quad (6)$$

Here $q_{\perp}^2 = q_x^2 + q_y^2$, and R_{\perp} , R_{\parallel} , R_0 , U are four K -dependent parameter functions. $U(\vec{K})$ is a 4-velocity with only a longitudinal spatial component:

$$U(\vec{K}) = \gamma(\vec{K}) (1, 0, 0, v(\vec{K})), \quad \text{with } \gamma = \frac{1}{\sqrt{1 - v^2}}. \quad (7)$$

Its value depends, of course, on the measurement frame. The ‘‘Yano-Koonin velocity’’ $v(\vec{K})$ can be calculated in an arbitrary reference frame from the second central space-time moments of $S(x, K)$ (for explicit expressions see Ref. [14]). It is, to a good approximation, the longitudinal velocity of the fluid element from which most of the particles with momentum \vec{K} are emitted [8, 14]. For sources with boost-invariant longitudinal expansion velocity the YK-rapidity associated with $v(\vec{K})$ is linearly related to the pair rapidity Y [14].

The other three YKP parameters do not depend on the longitudinal velocity of the observer. (This distinguishes the YKP form (6) from other parametrizations [10, 6, 7].) Their physical interpretation is easiest in terms of coordinates measured in the frame where $v(\vec{K})$ vanishes. There they are given by [8]

$$R_{\perp}^2(\vec{K}) = \langle \tilde{y}^2 \rangle, \quad (8)$$

$$R_{\parallel}^2(\vec{K}) = \langle (\tilde{z} - (\beta_{\parallel}/\beta_{\perp})\tilde{x})^2 \rangle - (\beta_{\parallel}/\beta_{\perp})^2 \langle \tilde{y}^2 \rangle \approx \langle \tilde{z}^2 \rangle, \quad (9)$$

$$R_0^2(\vec{K}) = \langle (\tilde{t} - \tilde{x}/\beta_{\perp})^2 \rangle - \langle \tilde{y}^2 \rangle / \beta_{\perp}^2 \approx \langle \tilde{t}^2 \rangle. \quad (10)$$

Here $\langle f(x) \rangle \equiv \int d^4x f(x) S(x, K) / \int d^4x S(x, K)$ denotes the (K -dependent) average over the source function $S(x, K)$, and $\tilde{x} \equiv x - \bar{x}(\vec{K})$ etc., where $\bar{x}(\vec{K}) = \langle x \rangle$ is (approximately) the source point with the highest intensity at momentum \vec{K} . R_{\perp} , R_{\parallel} and R_0 thus measure, approximately, the (K -dependent) transverse, longitudinal and temporal regions of homogeneity of the source in the local comoving frame of the emitter. The approximation in (9,10) consists of dropping terms which (for our model) vanish in the absence of transverse flow and were found in [14] to be small even for finite transverse flow. Note that it leads to a complete separation of the spatial and temporal aspects of the source. This separation is spoiled by sources with $\langle \tilde{x}^2 \rangle \neq \langle \tilde{x}^2 \rangle$. For our source this happens for non-zero transverse (in particular for large) transverse flow η_f , but for opaque sources where particle emission is surface dominated [19] this may be true even without transverse flow.

Since in the absence of transverse flow the β -dependent terms in (9) and (10) vanish and the source itself depends only on M_{\perp} , all three YKP radius

parameters then show perfect M_{\perp} -scaling. Plotted as functions of M_{\perp} , they coincide for pion and kaon pairs (see Fig. 5 in [17]). For non-zero transverse flow this M_{\perp} -scaling is broken by two effects: (1) The thermal exponent (4) receives an additional contribution proportional to $K_{\perp} = \sqrt{M_{\perp}^2 - m^2}$. (2) The terms which were neglected in the second equalities of (9,10) are non-zero, and they also depend on $\beta_{\perp} = K_{\perp}/E_K$. Both effects induce an explicit rest mass dependence and destroy the M_{\perp} -scaling of the YKP size parameters.

4 M_{\perp} -dependence of YKP radii and collective flow

Collective expansion induces correlations between coordinates and momenta in the source, and these result in a dependence of the HBT parameters on the pair momentum K . At each point in the source the local velocity distribution is centered around the average fluid velocity; two points whose fluid elements move rapidly relative to each other are thus unlikely to contribute particles with small relative momenta. Essentially only such regions in the source contribute to the correlation function whose fluid elements move with velocities close to the velocity of the observed particle pair. If the source expands rapidly and features large velocity gradients, these contributing “regions of homogeneity” will be small. Their size will be inversely related to the velocity gradients, scaled by a “thermal smearing factor” $\sqrt{T/M_{\perp}}$ which characterizes the width of the Boltzmann distribution [7].

Thus, for expanding sources, the HBT radius parameters are generically decreasing functions of the transverse pair mass M_{\perp} . The slope of this decrease grows with the expansion rate [13, 14]. Longitudinal expansion affects mostly the longitudinal radius parameter R_{\parallel} and the temporal parameter R_0 [14]; the latter is a secondary effect since particles from different points are usually emitted at different times, and a decreasing longitudinal homogeneity length thus also leads to a reduced effective duration of particle emission. The transverse radius parameter R_{\perp} is invariant under longitudinal boosts and thus not affected at all by longitudinal expansion. It begins to drop as a function of M_{\perp} , however, if the source expands in the transverse directions. The sensitivity of R_{\parallel} and R_0 to transverse flow is much weaker [14]. Transverse (longitudinal) flow thus affects mostly the transverse (longitudinal) regions of homogeneity. For a quantitative study see Fig. 6 in Ref. [17].

Unfortunately, the observation of an M_{\perp} -dependence of R_{\perp} by itself is not sufficient to prove the existence of radial transverse flow. It can also be created by other types of transverse gradients, e.g. a transverse temperature gradient [7, 12]. To exclude such a possibility one must check the M_{\perp} -scaling

of the YKP radii, i.e. the independence of the functions $R_i(M_\perp)$ ($i = \perp, \parallel, 0$) of the particle rest mass (which is not broken by temperature gradients). Since different particle species are affected differently by resonance decays, such a check further requires the elimination of resonance effects.

5 Resonance decays

Resonance decays contribute additional pions at low M_\perp ; these pions originate from a larger region than the direct ones, due to resonance propagation before decay. They cause an M_\perp -dependent modification of the HBT radii.

Quantitative studies [15, 16] have shown that the resonances can be subdivided into three classes with different characteristic effects on the correlator:

(i) Short-lived resonances with lifetimes up to a few fm/ c do not propagate far outside the region of thermal emission and thus affect R_\perp only marginally. They contribute to R_0 and R_\parallel up to about 1 fm via their lifetime; R_\parallel is larger if pion emission occurs later because for approximately boost-invariant expansion the longitudinal velocity gradient decreases as a function of time.

(ii) Long-lived resonances with lifetimes of more than several hundred fm/ c do not contribute to the measurable correlation and thus only reduce the correlation strength (the intercept at $q = 0$), without changing the shape of the correlator. The reason is that they propagate very far before decaying, thus simulating a very large source which contributes to the correlation signal only for unmeasurably small relative momenta.

(iii) There is only one resonance which does not fall in either of these two classes and can thus distort the form of the correlation function: the ω with its lifetime of 23.4 fm/ c . It contributes a second bump at small q to the correlator, giving it a non-Gaussian shape and complicating [16] the extraction of HBT radii by a Gaussian fit to the correlation function. At small M_\perp up to 10% of the pions can come from ω decays, and this fraction doubles effectively in the correlator since the other pion can be a direct one; thus the effect is not always negligible.

In a detailed model study [16] we showed that resonance contributions can be identified through the non-Gaussian features in the correlator induced by the tails in the emission function resulting from resonance decays. To this end one computes the second and fourth order q -moments of the correlator [16]. The second order moments define the HBT radii, while the kurtosis (the normalized fourth order moments) provide a lowest order measure for the deviations from a Gaussian shape. We found [16] that, at least for the model (1), a positive kurtosis can always be associated with resonance decay

contributions. Strong flow also generates a non-zero, but small and apparently always negative kurtosis (see Fig. 12 in [16]). Any M_{\perp} -dependence of R_{\perp} which is associated with a positive M_{\perp} -dependent kurtosis must therefore be regarded with suspicion; an M_{\perp} -dependence of R_{\perp} with a vanishing or negative kurtosis, however, cannot be blamed on resonance decays.

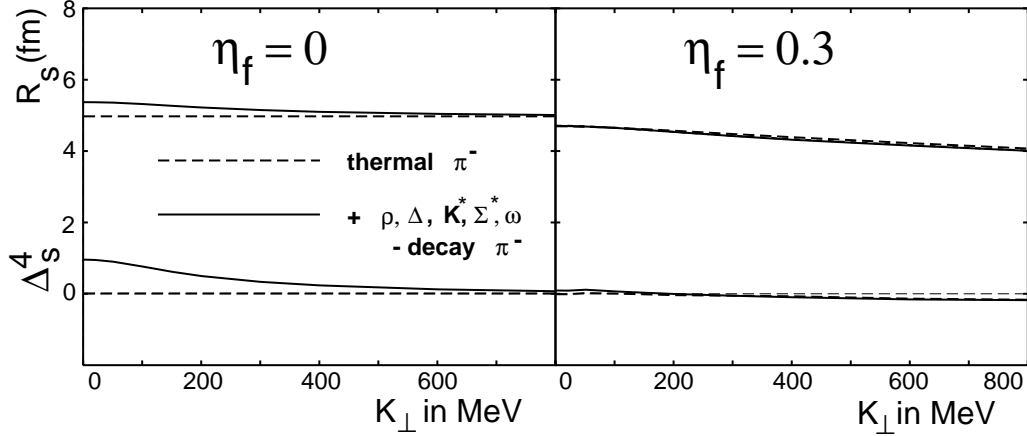


Fig. 1. The inverted q -variance R_{\perp} and the kurtosis Δ_{\perp} (the index s in the figure stands for “sideward”) at $Y = 0$ as functions of K_{\perp} . Left: $\eta_f = 0$ (no transverse flow). Right: $\eta_f = 0.3$. The difference between dashed and solid lines is entirely dominated by ω decays.

In our model, the first situation is realized for a source without transverse expansion (left panel of Fig. 1): At small M_{\perp} the ω contribution increases R_{\perp} by up to 0.5 fm while for $M_{\perp} > 600$ MeV it dies out. The effect on R_{\perp} is small because the heavy ω moves slowly and doesn’t travel very far before decaying. The resonance contribution is clearly visible in the positive kurtosis (lower curve). For non-zero transverse flow (right panel) there is no resonance contribution to R_{\perp} ; this is because for finite flow the effective source size for the heavier ω is smaller than for the direct pions, and the ω -decay pions thus always remain buried under the much more abundant direct ones. Correspondingly the kurtosis essentially vanishes; in fact, it is slightly negative, due to the weak non-Gaussian features induced by the transverse flow.

6 Analysis of Pb+Pb data

In Fig. 2 we show a numerical fit of the YKP radius parameters, using the expressions (8)-(10) with our model source (1), to data collected by the NA49

collaboration in 158 A GeV/c Pb+Pb collisions [20, 21]. Please note that this fit refers to only a single rapidity slice of the available data, and it does not include resonance decays. The fit result must therefore be taken with great care. A comprehensive simultaneous analysis of all single particle spectra and two-particle correlation data from Pb+Pb collisions is in progress.

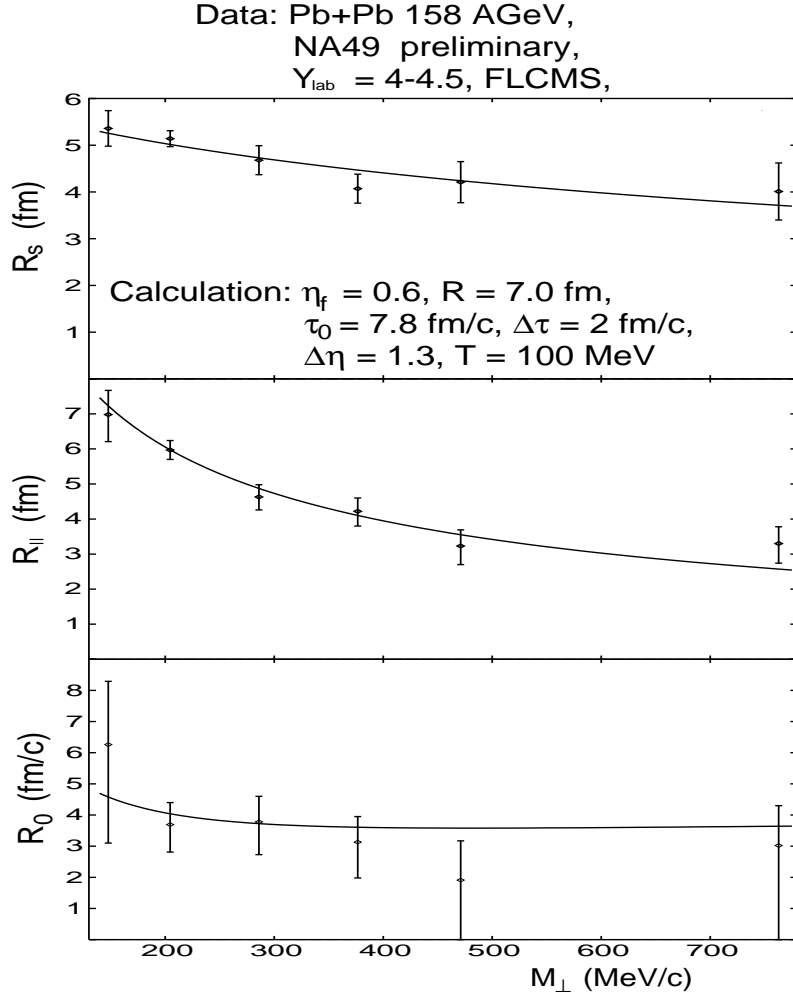


Fig. 2. R_{\perp} , R_{\parallel} and R_0 for 158 A GeV/c Pb+Pb collisions as functions of the transverse pair momentum. The data are from the NA49 Collaboration [21]. The lines are a fit with the model (1), with fit parameters as given in the figure.

After $\Delta\eta=1.2$ has been adjusted to reproduce the width of the pion rapidity distribution [21], the parameters τ_0 and $\Delta\eta$ are essentially fixed by the magnitude of R_{\parallel} and R_0 . The radius R is fixed by the magnitude of $R_{\perp}(K_{\perp} = 0)$ once the temperature T and transverse flow η_f are known. The M_{\perp} -dependence of

R_{\perp} fixes T and η_f , albeit not independently: essentially only the combination $\eta_f \sqrt{M_{\perp}/T}$, i.e. the velocity gradient divided by the thermal smearing factor, can be extracted [8, 21]. This is similar to the single particle spectra whose M_{\perp} -slopes determine only an effective bluishifted temperature, $T_{\text{eff}} = T \sqrt{\frac{1+\bar{v}_f}{1-\bar{v}_f}}$ [1]. The correlations between T and η_f are, however, exactly opposite in the two cases: for a fixed spectral slope T must be decreased if η_f increases while a fixed M_{\perp} -slope of R_{\perp} requires decreasing values of η_f if T is reduced [21]. The combination of single-particle spectra and two-particle correlation thus allows for a separate determination of T and η_f .

For the fit in Fig. 2 the freeze-out temperature was set by hand to $T = 100$ MeV. The resulting flow parameter $\eta_f=0.6$ corresponds to an average transverse flow velocity $\bar{v}_f=0.58$. This combination of T and η_f results in single-particle spectra with roughly the right shape. Fitting R_{\perp} with higher temperatures results in larger η_f -values which leads to single particle spectra which are much too flat.

Let us discuss in more detail the numbers resulting from this fit. First, the transverse size parameter $R=7$ fm is surprisingly large. Resonance contributions are not expected to reduce it by more than 0.5 fm [16]. The transverse flow correction to R_{\perp} is appreciable, resulting in a visible transverse homogeneity length of only about 5.5 fm at small K_{\perp} , but even this number is large. $R=7$ fm corresponds to an r.m.s. radius $r_{\text{rms}} = \sqrt{\langle \tilde{x}^2 + \tilde{y}^2 \rangle} \approx 10$ fm of the pion source, to be compared with an r.m.s. radius $r_{\text{rms}}^{\text{Pb}} = 1.2 \times A^{1/3}/\sqrt{5}$ fm = 3.2 fm for the density distribution of the original Pb nucleus projected on the transverse plane. This implies a transverse expansion of the reaction zone by a linear factor 3. That we also find a large transverse flow velocity renders the picture consistent. The longitudinal size of the collision region at the point where the pressure in the system began to drive the transverse expansion is less clear; assuming a similar expansion factor 3 in the beam direction (although we know from the fit that the longitudinal expansion velocity is much bigger than the transverse one) we conclude that the fireball volume must have expanded by at least a factor $3^3 = 27$ between the onset of transverse expansion and freeze-out! This is the clearest evidence for strong collective dynamical behaviour in ultra-relativistic heavy-ion collisions so far.

The local comoving energy density at freeze-out can be estimated from the fitted values for T and η_f . The thermal energy density of a hadron resonance gas at $T = 100$ MeV and moderate baryon chemical potential is of the order of 50 MeV/fm³. The large average transverse flow velocity of $\langle v_f \rangle \approx 0.58$ implies that about 50% flow energy must be added in the lab frame. This

results in an estimate of about $0.050 \text{ GeV}/\text{fm}^3 \times 1.5 \times 27 \approx 2 \text{ GeV}/\text{fm}^3$ for the energy density of the reaction zone at the onset of transverse expansion. This is well above the critical energy density $\epsilon_{\text{cr}} \leq 0.9 \text{ GeV}/\text{fm}^3$ predicted by lattice QCD for deconfined quark-gluon matter [22]. Whether this energy density was thermalized is, of course, a different question. In any case it must have been accompanied by transverse pressure, because otherwise transverse expansion could not have been initiated.

7 Conclusions

I hope to have shown that

- two-particle correlation functions from heavy-ion collisions provide valuable information both on the geometry **and** the dynamical state of the reaction zone at freeze-out;
- a comprehensive and simultaneous analysis of single-particle spectra and two-particle correlations, with the help of models which provide a realistic parametrization of the emission function, allows for an essentially complete reconstruction of the final state of the reaction zone, which can serve as a reliable basis for theoretical back-extrapolations towards the interesting hot and dense early stages of the collision;
- simple and conservative estimates, based on the crucial new information from HBT measurements on the large transverse size of the source at freeze-out and using only energy conservation, lead to the conclusion that in Pb+Pb collisions at CERN, before the onset of transverse expansion, the energy density exceeded comfortably the critical value for the formation of a color deconfined state of quarks and gluons.

Acknowledgements: This work was supported by grants from DAAD, DFG, NSFC, BMBF and GSI. The results reported here were obtained in collaboration with S. Chapman, P. Scotto, B. Tomášik, U. Wiedemann, and Y.-F. Wu, to whom I would like express my thanks. I gratefully acknowledge many discussions with H. Appelshäuser, T. Csörgő, D. Ferenc, M. Gaździcki, S. Schönfelder, P. Seyboth, and A. Vischer.

References

- [1] K.S. Lee and U. Heinz, Z. Phys. **C43** (1989) 425; K.S. Lee, U. Heinz and E. Schnedermann, Z. Phys. **C48** (1990) 525; E. Schnedermann and U. Heinz, Phys. Rev. Lett. **69** (1992) 2908; E. Schnedermann, J. Sollfrank and U. Heinz, Phys. Rev. **C48** (1993) 2462; E. Schnedermann and U.

- Heinz, Phys. Rev. **C50** (1994) 1675; U. Heinz, in *Hot Hadronic Matter: Theory and Experiment*, Eds: J. Letessier et al., NATO ASI Series **B346**, Plenum, New York, 1995, p.413.
- [2] J. Stachel et al., [E814 collaboration], Nucl. Phys. **A566** (1994) 183c; P. Braun-Munzinger et al., Phys. Lett. **B344** (1995) 43.
- [3] See proceedings of *Quark Matter 96*, Nucl. Phys. **A610** (1996), in press (in particular contributions by Y. Akiba, N. Herrmann, P. Jones, R. Lacasse, J. Stachel, and Nu Xu).
- [4] A. Leonidov, M. Nardi and H. Satz, Z. Phys. **C**, in press.
- [5] S. Esumi, U. Heinz, and N. Xu, submitted to Phys. Lett. **B**.
- [6] M. Herrmann and G.F. Bertsch, Phys. Rev. **C51** (1995) 328.
- [7] S. Chapman, P. Scotto and U. Heinz, Phys. Rev. Lett. **74** (1995) 4400; and Heavy Ion Physics **1** (1995) 1.
- [8] S. Chapman, J.R. Nix and U. Heinz, Phys. Rev. **C52** (1995) 2694.
- [9] S.V. Akkelin and Y.M. Sinyukov, Phys. Lett. **B356** (1995) 525.
- [10] S. Pratt, Phys. Rev. Lett. **53** (1984) 1219; Phys. Rev. **D33** (1986) 1314.
- [11] A.N. Makhlin and Yu.M. Sinyukov, Z. Phys. **C39** (1988) 69.
- [12] T. Csörgő and B. Lörstad, Phys. Rev. **C54** (1996) 1396.
- [13] U.A. Wiedemann, P. Scotto and U. Heinz, Phys. Rev. **C53** (1996) 918.
- [14] U. Heinz et al., Phys. Lett. **B382** (1996) 181; Wu Y.-F. et al., nucl-th/9607044.
- [15] B.R. Schlei et al., Phys. Lett. **B293** (1992) 275; J. Bolz et al., *ibid.* **B300** (1993) 404; Phys. Rev. **D47** (1993) 3860.
- [16] U.A. Wiedemann and U. Heinz, nucl-th/9610043, subm. to Phys.Rev. Lett.; and nucl-th/9611031, subm. to Phys. Rev. **C**.
- [17] U. Heinz, in *Correlations and Clustering Phenomena in Subatomic Physics*, (M.N. Harakeh et al., eds.), NATO ASI Series B, Plenum, 1996, in press (nucl-th/9609029).
- [18] E. Shuryak, Phys. Lett. **B44** (1973) 387; Sov. J. Nucl. Phys. **18** (1974) 667.
- [19] H. Heiselberg and A.P. Vischer, nucl-th/9609022.
- [20] NA49 Coll., K. Kadija et al., in [3]; H. Appelshäuser, PhD thesis, Univ. Frankfurt (1996).
- [21] S. Schönfelder, PhD thesis, MPI für Physik, München (1996).
- [22] F. Karsch, lectures given at Kloster Banz, Oct. 8-10, 1996; and this volume.